ELSEVIER

Thin Solid Films 413 (2002) 203–211

thin solid films

www.elsevier.com/locate/tsf

Electrical and optical properties of tin-doped CdO films deposited by atmospheric metalorganic chemical vapor deposition

Zhiyong Zhao[1], D.L. Morel, C.S. Ferekides*

Department of Electrical Engineering, University of South Florida, Tampa, FL 33620, USA

Received 11 December 2001; received in revised form 25 March 2002; accepted 26 March 2002

Abstract

Highly conductive and transparent tin-doped CdO:Sn were deposited via atmospheric metalorganic chemical vapor deposition. Dimethylcadmium (DMCd), tetramethyltin (TMT), and O_2 were used to deposit the CdO:Sn films. The structural, electrical, and optical properties of the fabricated films were influenced by the partial pressures of DMCd and TMT, substrate temperature, film thickness, and annealing conditions. A sheet resistance of 14–17 Ω/sq was obtained for as-deposited CdO:Sn films with a thickness of 120–150 nm. The high conductivity of the films was mainly due to their high carrier concentration ($2–3\times10^{21}$/cm^3) and moderate mobility (12–13 cm^2/V s). The transmission of the films in the visible range was high (80–95%) and shifted towards the blue region due to the Moss-Burstein (M-B) effect. The films exhibited direct and indirect band-to-band transitions, which corresponded to optical bandgaps of $\sim$3.0 and $\sim$2.5 eV, respectively. The electro-optical properties of as-deposited CdO:Sn films were further improved by post-deposition annealing. A resistivity value of $1.4–1.6\times10^{-4}$ Ω cm has been obtained after annealing in He and H_2 ambients, which is the lowest value ever reported for CdO films.

Keywords: Cadmium oxide; Metalorganic chemical vapor deposition; Optical properties; Electrical properties

1. Introduction

Due to the nature of their excellent electrical conductivity and optical transmission, transparent conductive oxides (TCOs) have been used in many applications, such as low-e windows, flat panel displays, photovoltaic devices, smart windows, and deicing heaters on vehicles. Tin oxide (SnO_2), zinc oxide (ZnO), and indium tin oxide (ITO) have been the dominant TCO materials for these applications. For different applications, the requirements for choosing a TCO material may differ. The TCOs used in solar cells should be highly transparent to the solar spectrum, have low electrical resistivity [1], be stable under H-plasma, and have a suitable structure in particular for a-Si solar cells. For other applications additional criteria can be of importance, which include physical, chemical, and thermal durability, etchability, work function, uniformity, toxicity, and cost [2].

Although CdO was the very first reported transparent conducting film made by oxidation of sputtered metallic cadmium [3], it has not been extensively studied compared to other TCOs due to its relatively small bandgap. A variety of thin film deposition techniques, like spray pyrolysis [4–6], ion beam sputtering [6], chemical bath deposition [7], activated reactive evaporation [8], thermal oxidation [9], reactive sputtering [10,11], and sol–gel [12] have been employed to produce CdO films.

CdO is an n-type semiconductor with a NaCl structure. Nonstoichiometric undoped CdO thin films usually exhibit low resistivity due to native defects of oxygen vacancies and cadmium interstitials. Hence, low-resistivity films can be obtained by controlling these native defects. Nevertheless, attempts have been made to extrinsically dope CdO films with In and Cu [13], because the extrinsic donors are more stable than the intrinsic ones. To date, however, no CdO films have been made meeting both the high conductivity and transmittance requirements for solar cell applications.

In this study, tin-doped CdO (CdO:Sn) was deposited by atmospheric pressure metalorganic chemical vapor

*Corresponding author. Tel.: +1-813-974-4818.
E-mail address: ferekide@eng.usf.edu (C.S. Ferekides).
[1] Present address: Microcoating Technologies of Atlanta, GA, USA.

0040-6090/02/$ - see front matter © 2002 Elsevier Science B.V. All rights reserved.
PII: S0040-6090(02)00344-9

deposition and its structural, electrical, and optical properties were investigated. The results showed that highly transparent and conductive CdO:Sn films are promising for photovoltaic applications.

2. Experimental

In recent years, the metalorganic chemical vapor deposition (MOCVD) process has received increasing attention for the growth of thin film semiconductors because of certain distinct advantages largely associated with the ease of handling the metal sources and especially its potential for large scale coatings at high growth rates. The horizontal reactor MOCVD system used in the present work has been described in detail elsewhere [14]. A Eurotherm 818 temperature controller is used to control the graphite susceptor temperature that can be raised up to 800 °C, as measured by a thermocouple inserted inside the susceptor. The deposition temperature can be stabilized within ±1 °C. The deposition reaction was studied over the temperature range of 200–300 °C at atmospheric pressure. The reactor inlets (manifold) are connected to gas lines, which transport various gases. The flow rates are independently controlled by UNIT mass-flow controllers. The tetramethyltin (TMT) and dimethylcadmium (DMCd) stainless bubblers were maintained at 17 and 27 °C, respectively, in temperature-controlled baths. It was assumed that the helium bubbling through the liquid TMT and DMCd was saturated with the vapors, hence the mass of MO transported to the reactor can be controlled either by the flow rate through the liquid or by changing the bath temperature.

Tin-doped cadmium oxide was prepared using O_2, DMCd, and TMT as precursors, and high purity (99.999%) helium was used as carrier gas. Corning 7059 glass was used as the substrate.

The experimental procedure used to prepare a typical film was as follows:

a. 7059 glass substrates were cleaned and placed on the graphite susceptor;
b. the reactor was then purged with helium while the substrate temperature was raised to the desired deposition temperature;
c. once the substrates reached the desired temperature the reactant gases were introduced into the reactor to start the deposition process;
d. after the deposition was completed, helium flow through the reactor was maintained until the susceptor/substrates cooled to room temperature.

The thickness uniformity of the CdO:Sn films is affected by the gas flow rates, substrate temperature, and reaction rate, etc. Because DMCd is very reactive with O_2 even at room temperature, high purity He (99.999%) was used to dilute the precursor gas using a separate line, which was also used to improve the film uniformity. The main-line carrier gas (He) was used to keep the film thickness uniform within ±10%.

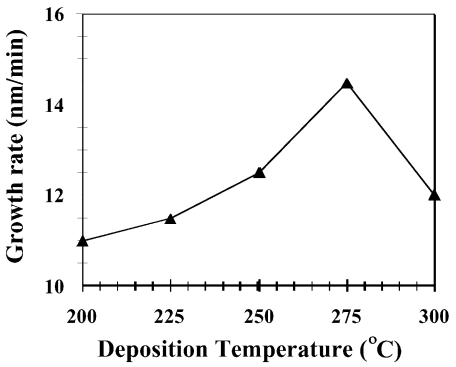

Fig. 1. Growth rate as a function temperature.

The films were characterized by optical, electrical, and structural measurements.

The room temperature sheet resistance was measured either with a four-point probe or by the Van der Pauw technique. The Hall measurement was carried out in the four-probe configuration using indium dot contacts (silver was also used as ohmic contacts for CdO [10]) in a magnetic field of 0.552 T. For each sample, three currents were used to measure the Hall voltage, and the average of the three Hall coefficients was used to calculate the carrier concentration and mobility.

An alpha-step 200 (Tencor Instruments) profilometer was used to obtain the film thickness by measuring a well-defined step height (as-deposited CdO can be easily etched in dilute HCl).

Optical transmission was measured using a Varian Cary 17-D spectrophotometer with a glass substrate positioned in the reference beam sample chamber.

The structural and compositional properties were characterized by X-ray diffraction (XRD), scanning electron microscopy (SEM), and energy dispersive spectrometry (EDS). The XRD measurements were carried out on a Scintag XDS-2000 θ–2θ system with CuKα radiation (λ = 0.15418 nm) at 40 keV and 35 mA; the diffraction spectra of the films were obtained by scanning 2θ in the range of 30–60°. SEM micrographs were taken on a JEOL JSM 840 SEM system. EDS analysis was performed using a Tracor Northern (Noran) TN550 Energy Dispersive X-ray Spectrometer.

3. Results and discussion

3.1. Film growth rate

The prepared CdO:Sn films were found to be pinhole free and have strong adherence to the glass substrates. The growth rates were calculated from the ratio of film thickness in the middle of the substrate to deposition time, and have been found to have a near linear

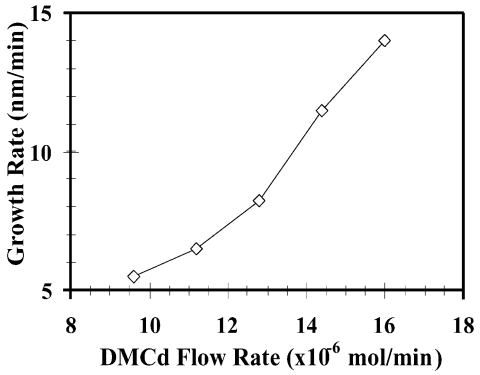

Fig. 2. Growth rate as a function of the flow rate of DMCd.

dependence on the substrate temperature between 200 and 275 °C, and dropped at 300 °C (Fig. 1). The flow rates of DMCd, TMT, and O_2 were held constant at 1.6×10^{-5}, 1.45×10^{-4}, and 4.45×10^{-2} mol/min, respectively. At low temperatures, in the range of 200–275 °C, the reactions to form film precursors were slow, i.e. 'surface limited', so the deposition was slow and had a linear relation with temperature. The films were found to have a $\pm10\%$ uniformity over a 10×10 cm^2 area. At high temperatures (300 °C), gas-phase reactions were fast, and the film precursors depleted in the gas phase, which resulted in a lower growth rate and poorer uniformity.

The growth rate of CdO increases monotonically with the DMCd flow rate as depicted in Fig. 2, where the films were deposited at 250 °C with a TMT flow rate of 1.45×10^{-4} mol/min and an oxygen flow rate of 4.45×10^{-2} mol/min. This is due to the fact that, within the above flow rates, oxygen is in excess and therefore any additional DMCd readily reacts with it to from CdO. A slight change in the deposition rate was also observed when the amount of TMT introduced in the reactor was increased.

3.2. Film structure and composition

Polycrystalline (PX) CdO powder of random orientation shows four strong diffraction peaks associated with {1 1 1}, {2 0 0}, {2 2 0} and {3 3 1} reflections with *d* values of 0.2712, 0.2349, 0.1661 and 0.1416 nm and relative intensities of 100, 88, 43 and 28, respectively.

Fig. 3 shows the XRD spectra of CdO:Sn films deposited at temperatures in the range of 200–300 °C (the XRD pattern of CdO deposited at 250 °C using the same MOCVD system is also given for comparison). The observed diffraction peaks were at 33.10, 38.44 and 55.48°, respectively for the film deposited at 250 °C, as compared with 33.03, 38.32 and 55.31°, respectively, for PX CdO powder. The shifts of diffraction peaks in the CdO:Sn films are most likely due to a slight change

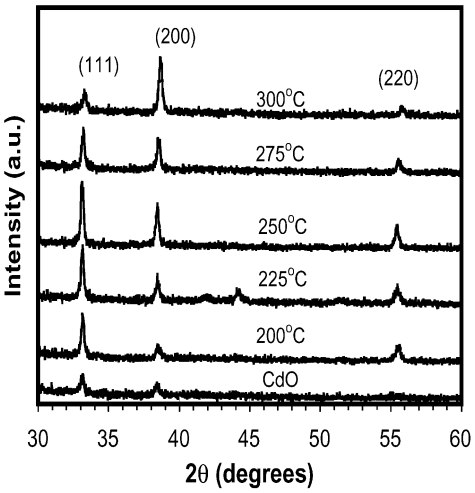

Fig. 3. XRD patterns of films deposited at different temperatures. The undoped CdO film was prepared at 250 °C.

in the lattice parameter associated with (1) oxygen vacancies, (2) Sn substitutes, and/or (3) stress. The ratios of the three major XRD peaks of the films, i.e. (1 1 1), (2 0 0) and (2 2 0), are plotted in Fig. 4. It can be seen that the (2 0 0) orientation is enhanced as the deposition temperature increases. The films show stronger (1 1 1) orientations at temperatures below 275 °C, and a stronger (2 0 0) orientation at 300 °C. The intensity of the (2 2 0) orientation shows a slight dependence on temperature and appears to reach a maximum at 250 °C. Similar dependence of preferred orientation of activated reactive evaporated CdO on substrate temperatures has been reported elsewhere [8].

When the flow rate of TMT was increased, the (1 1 1) orientation appeared to be enhanced as shown in Fig. 5, which suggests that within the range of concentrations studied in this work, as more tin is incorporated into the films their crystallinity improves. The films in Fig. 5 were all deposited at 250 °C with a DMCd flow rate of 1.6×10^{-5} mol/min and an oxygen flow rate of 4.45×10^{-2} mol/min.

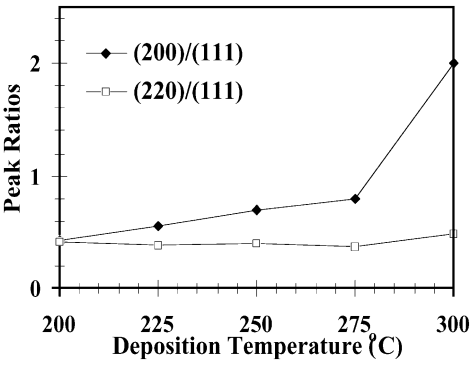

Fig. 4. Intensity ratios of the XRD peaks (2 0 0)/(1 1 1) and (2 2 0)/(1 1 1) as functions of substrate temperature.

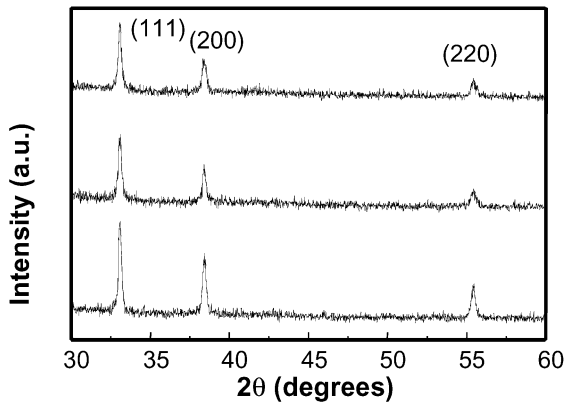

Fig. 5. XRD spectra of films deposited at different TMT flow rates.

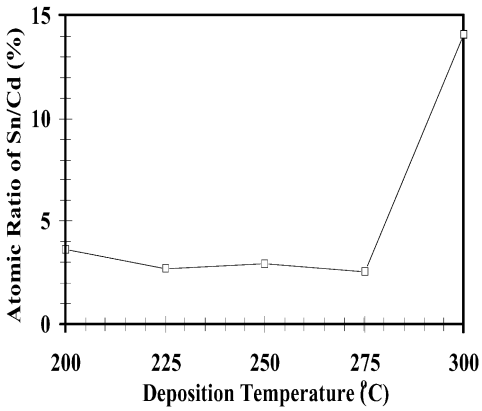

Fig. 6. Atomic ratio of Sn/Cd of the films deposited at different temperatures.

The structural parameters of the films depicted in Fig. 3 have been calculated and are reported in Table 1. The lattice parameter (a) was calculated using the Bragg's formula and Nelson–Riley function. The vertical crystallite size (D) was calculated from the Scherrer's formula. The dislocation density (ϕ) was evaluated using the formula suggested by Williamson and Smallman [15], which is $\phi = n/D^2$, where n is a factor which equals unity giving minimum dislocation density. The films deposited at 250 °C had the largest vertical grain size and lowest dislocation density, which is in good agreement with the highest mobility values obtained from Hall measurements (to be discussed below).

SEM was also used to characterize the CdO:Sn films. The film surface was found to be relatively smooth (indicated from thickness/roughness measurements with a surface profilometer). All CdO:Sn films showed PX structure with textured surfaces. The film deposited at 200 °C showed weak PX morphology, primarily due to the fact that the crystallization temperature of amorphous CdO films is 225 °C [16]. The film deposited at 275 °C had the smallest grain size around 100–150 nm. Fig. 6 shows the atomic ratio Sn/Cd obtained from energy dispersive X-ray spectrometry measurements for the films deposited at various temperatures. It is seen that the film deposited at 275 °C had the least amount of tin. Based on these results it is suggested that the structural properties of the films are primarily affected by the deposition temperature and the amount of incorporated tin.

Table 1
Calculated microstructural parameters associated with the MOCVD CdO:Sn films

T_{sub} (°C)	A (Å)	D (nm)	ϕ ($\times 10^{11}$ lines/cm^2)
ASTM	4.6953		
200	4.682	29.9	1.118
225	4.684	31.57	1.003
250	4.686	35.88	0.777
275	4.678	31.23	1.025
300	4.662	24.02	1.733

3.3. Electrical properties

The sheet resistance and resistivity as measured by four-point probe are shown in Fig. 7. It is clear that the resistivities of the films strongly depend on the deposition temperature. The lowest sheet resistance and resistivity were obtained for the films deposited at the substrate temperature of 250 °C, which were 17.4 Ω/sq and 2.13×10^{-4} Ω cm, respectively.

All samples showed n-type conductivity as determined by their negative Hall coefficients. The carrier concentration and mobility of the as-deposited CdO:Sn films are shown in Fig. 8. The carrier concentration of the films was remarkably high in the range of 1.7–3.6×10^{21}/cm^3, which is beneficial in lowering the fundamental absorption edge [16] and increasing their optical bandgaps. However, high carrier concentrations

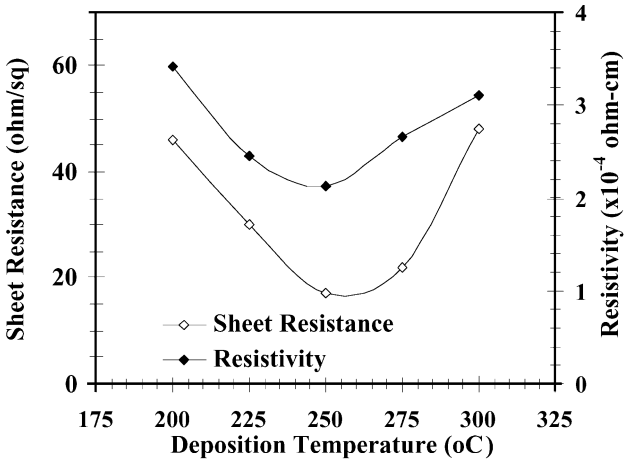

Fig. 7. Sheet resistance and resistivity results of CdO:Sn films fabricated at different temperatures.

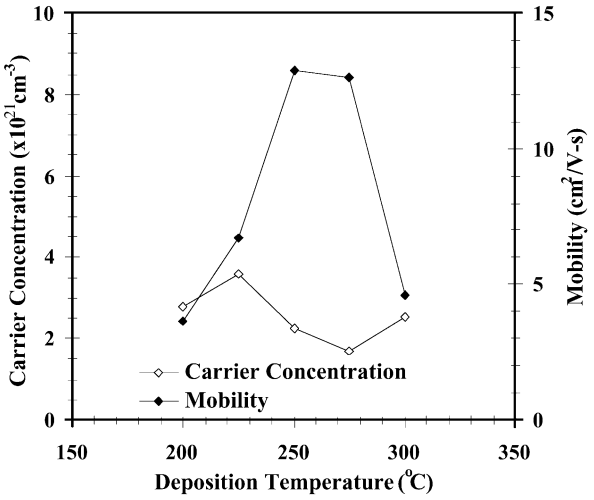

Fig. 8. Carrier concentration and mobility of CdO:Sn films deposited at different temperatures.

also lead to larger free-carrier absorption (absorption coefficient is proportional to the carrier concentration).

The mobilities were in the range of 3.6–12.8 $cm^2/V\,s$, and the highest mobility of 12.8 $cm^2/V\,s$ was found for the film deposited at 250 °C. The moderate mobility could be attributed to the combined contributions of various scattering mechanisms, i.e. ionized impurity scattering, grain boundary scattering and lattice scattering, with the grain boundary scattering most likely being the dominant mechanism.

The deposition temperature strongly influences both the gas-phase reaction and the movement of dopant atoms to positions in which they are electrically active. The doping efficiency, defined as the ratio of the number of free electrons in the films to the tin concentration, gives the fraction of tin atoms that are electrically active in the film. The doping efficiency (η_{DE}) can be calculated from the free-electron concentration of the film, the tin percentage, and the CdO density. A tin atom replacing a cadmium atom in the CdO crystal can yield two free electrons, while a tin atom occupying an interstitial position could contribute up to four free electrons. Table 2 shows the doping efficiency of the CdO:Sn films as a function of deposition temperature. Each tin atom was assumed to provide two electrons.

Table 2
Doping efficiency (η_{DE}) comparison of the CdO:Sn films grown at different deposition temperatures

Deposition temperature (°C)	N_{Sn} ($\times 10^{21}$ atoms/cm^3)	N_e ($\times 10^{21}$/cm^3)	η_{DE} (%)
200	3.492	2.77	103.3
225	2.657	3.59	175.9
250	3.237	2.24	102.4
275	3.264	1.68	88.4
300	12.51	2.54	26.7

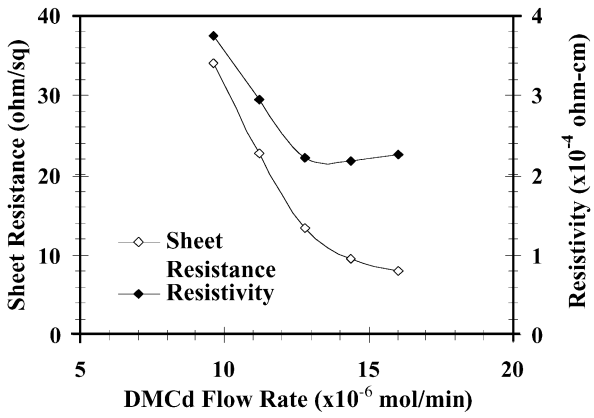

Fig. 9. Sheet resistance and resistivity of CdO:Sn films at 250 °C with varied flow rates of DMCd.

Doping efficiency above 100% may result either from the contribution of more than two free electrons from some tin atoms (interstitials), cadmium interstitials, and/or oxygen vacancies. The amount of incorporated tin is also given in Table 2. More tin appears to be incorporated into the films with increasing temperature from 225 to 300 °C. The resistivity of the films decreased with increasing flow rate of DMCd from 0.96×10^{-5} to 1.28×10^{-5} mol/min as shown in Fig. 9, and little change was observed as the DMCd flow rate beyond 9.6×10^{-6} mol/min. Since higher flow rate of DMCd yields a higher growth rate, a flow rate of 1.6×10^{-5} mol/min was chosen as the optimum experimental condition. The sheet resistance decreased with increasing TMT flow rate, and saturated at 1.45×10^{-4} mol/min, as shown in Fig. 10. A flow rate of 1.45×10^{-4} mol/min for TMT was selected as standard experiment condition.

The dependence of the electrical properties and surface morphology on the film thickness was also evaluated. The films were deposited at the same deposition conditions (250 °C) with deposition time being the only variable. Fig. 11 shows the results of Hall measurements

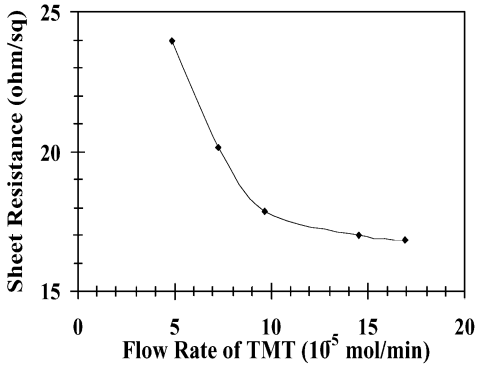

Fig. 10. Sheet resistance of CdO:Sn films at 250 °C with different flow rates of TMT.

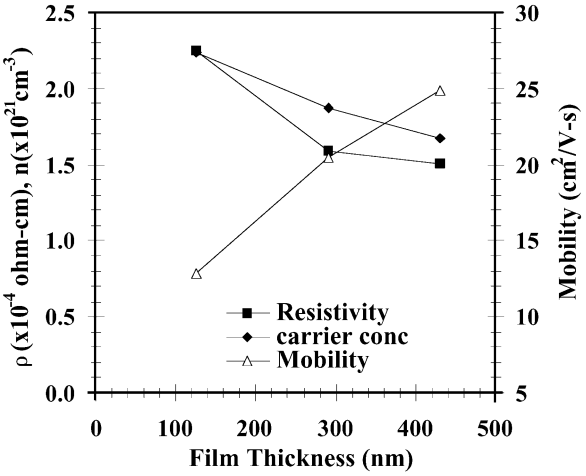

Fig. 11. Resistivity (ρ), mobility (μ), and carrier concentration (n) vs. film thickness.

as a function of thickness. Both the resistivity and carrier concentration decreased with increasing film thickness, while the mobility increased with film thickness.

The SEM images showed that the shape of the rock-like morphology does not change with film thickness but the grain size becomes larger as the film thickness is increased. This result indicates that the grains are not uniform in the thickness direction, but are smaller initially and grow larger as the films become thicker. Grain boundary scattering of free electrons in thicker films is less than in thinner films because of the larger crystallite size. Since the conductivity (σ) is inversely proportional to the electron scattering frequency, $\gamma(\sigma = N_e e^2/m_e^*\gamma)$, the conductivity of thicker films is higher than that of thinner films.

3.4. Optical properties

3.4.1. Transmission

The specular transmittance of CTO is expected to depend mainly on three factors: (1) oxygen deficiency, (2) surface roughness (surface scattering reduces the specular transmission, which in turn depends on the grain size and shape), and (3) impurity centers.

The specular transmission of films was measured with a blank glass as reference. The transmission spectra of the films deposited at different temperatures are shown in Fig. 12. The transmission of undoped CdO deposited at 250 °C is also shown in the same figure. It is seen that the transmission improved significantly after tin doping due to an apparent shift in the absorption edge.

All the as-deposited films exhibited high transmittance (80–95%) in the visible region, and showed a fundamental absorption edge in the range of 400–480 nm. It should be noted that the films had high transmission in the range of 500–600 nm in which the solar spectrum is maximum.

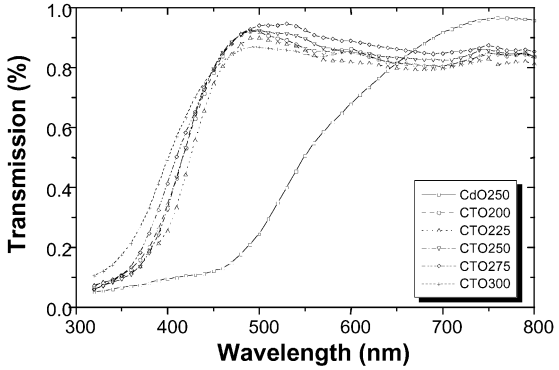

Fig. 12. Optical transmission spectra in the visible region of CdO:Sn films deposited at different temperatures.

3.4.2. Optical bandgap

The optical bandgap of the films was estimated by extrapolation of the linear portion of $(\alpha h\nu)^{1/2}$ and $(\alpha h\nu)^2$ vs. $h\nu$, respectively, where α is the absorption coefficient, and $h\nu$ the photon energy.

The changes in the bandgap were relatively small for films deposited at different temperatures, and were in the range of 3.0–3.2 and 2.52–2.56 eV, respectively, for direct and indirect band-to-band transitions. The values of $(\alpha h\nu)^{1/2}$ and $(\alpha h\nu)^2$ as functions of $h\nu$ for CdO:Sn films deposited at 250 °C are shown in Fig. 13. A direct bandgap of 3.0 eV and indirect bandgap 2.5 eV are obtained from the plots. Band structure calculations have predicted the existence of two indirect gaps at 1.2 and 0.8 eV [17], at 1.11 and 0.95 eV [18], at 1.18 and 1.12 eV [19], or at 0.9 ± 0.1 eV [20]. The direct value is 2.18 ± 0.04 eV [20] or 2.38 eV [21]. The higher direct

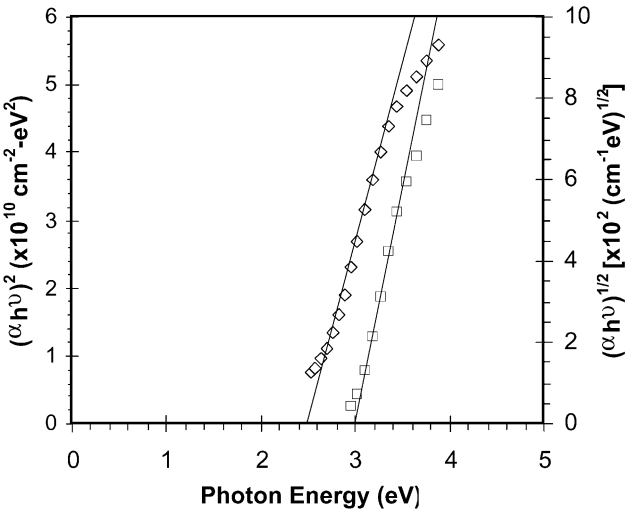

Fig. 13. Plots of $(\alpha h\nu)^2$ and $(\alpha h\nu)^{1/2}$ vs. $h\nu$ for the films deposited at 250 °C.

value in the present work is believed to be partly due to the Moss–Burstein (M-B) effect. The high free carrier absorption of CdO could have masked a second gap [20].

The blue-shift of the absorption edge has been generally interpreted by the M-B effect. The absorption edge shift in an n-type semiconductor is given by:

$$\Delta E^{\mathrm{BM}} = (\hbar^2/2m_{\mathrm{vc}}^*)(3\pi^2)^{2/3}N^{2/3} \ (\mathrm{eV}) \quad (1)$$

Where $\hbar$ is the Planck constant, m_{vc}* the reduced effective mass ($1/m_{\mathrm{vc}}^* = 1/m_{\mathrm{c}}^* + 1/m_{\mathrm{v}}^*$), and N the free carrier (which is electrons for n-type semiconductors) concentration.

At high carrier concentrations above the Mott critical density, the electronic states of the crystal are modified because of carrier–carrier interaction and carrier–impurity interaction, which can lead to a narrowing of the bandgap. According to Wolff [22], in heavily n-doped semiconductors the conduction band is shifted downward by a quantity equal to ΔE^{EX}

$$\Delta E^{\mathrm{EX}} = (q/2\pi\varepsilon_0\varepsilon_r)(3/\pi)^{1/3}N^{1/3} \ (\mathrm{eV}) \quad (2)$$

Where q is the electron charge, ε_0 the permittivity of vacuum, and ε_{r} the dielectric constant of the semiconductor. At high concentrations in the order of $10^{20}/\mathrm{cm}^3$, this band shrinkage effect begins to be competitive with the M-B shift. The expected absorption edge shift is therefore calculated by

$$\Delta E = \Delta E^{\mathrm{BM}} - \Delta E^{\mathrm{EX}} \ (\mathrm{eV}) \quad (3)$$

In Eqs. (1)–(3), since the carrier concentration, N, is known for a specific film, the effective mass of electrons can be calculated from the bandgap of the nondegenerate material and ΔE obtained from the optical measurements. Calculations showed that the effective mass of electrons was in the range of 0.4–0.6 m_0 for CdO:Sn films deposited at 225–300 °C, where m_0 is the rest electron mass. The higher effective mass value than that of nondegenerate CdO is believed to be due to the considerably high carrier concentration [23].

The ratio recording technique was also used to evaluate the optical bandgap of as-deposited films. A thinner film was used as a reference instead of glass. The optical bandgaps were found to be 3.05 and 2.62 eV for direct and indirect transitions, respectively, which are very close to what was obtained from the normal transmission technique.

Higher bandgaps are always required for TCO films used in solar cell applications. The optical bandgap of CdO obtained in this work is higher than the values reported by other researchers, i.e. 2.35–2.5 eV [4], 2.4 [6], 2.2 [7], and 2.55–2.68 [10].

3.5. Figure of merit

Haacke's definition of figure of merit $\phi_{\mathrm{TC}} = T^{10}/R_{\mathrm{s}}$ was used to evaluate the optical and electrical properties of the CdO:Sn films, where T is the transmission and R_{s} the sheet resistance of the film being evaluated.

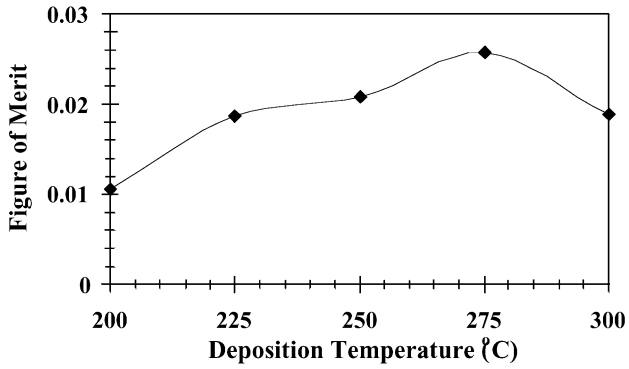

Fig. 14. Figure of merit evaluation of as-deposited CdO:Sn films.

The transmission at 500 nm (solar radiation maximum) was used to calculate the figure of merit of the films. The results are shown in Fig. 14. It is seen that as-deposited films had a high figure of merit of the order of $10^{-2}/\Omega$, with the film deposited at 275 °C having the highest figure of merit. Transparent conducting oxide films should have high transmission and conductivity, but in various applications of TCO films, either the electrical or optical properties are more critical. In those cases a different form of figure of merit may be needed to describe the film's electro-optical properties.

3.6. Annealing effects

Post-deposition annealing has been noted to be helpful in improving a film's electro-optical properties. The as-grown CdO:Sn films deposited at 250 °C have been annealed in He ambient in the presence of CdS at temperatures up to 575 °C, and H_2 ambient at temperatures up to 400 °C, respectively [27]. Annealing in H_2 was limited to lower temperatures due to the fact that above 350 °C the films became darker suggesting loss of oxygen and conversion to metallic cadmium. Both the sheet resistance and optical transmission improved after annealing, and a resistivity as low as 1.4–1.6×10^{-4} Ω cm has been achieved for both annealing conditions. This value is, to our knowledge, the lowest ever reported for undoped and doped CdO films, and comparable to the state-of-the-art resistivity values of ITO, ZnO doped with Ga or Al, and Cd_2SnO_4 films. As a comparison, the electrical and optical properties of CdO films fabricated by different researchers are summarized in Table 3. An optical bandgap of 3.35 eV was achieved for CdO films annealed in H_2, and is believed to be the highest ever reported value for this material.

Furthermore, Hall measurements carried out on the annealed films revealed that two different mechanisms govern the improvement after He annealing and H_2

Table 3
A summary of electrical and optical properties of CdO films prepared by various researchers

Materials	ρ (Ω cm)	μ ($cm^2/V\,s$)	N ($1/cm^3$)	E_g (eV)	Method[a]	Reference
CdO	2.1×10^{-3}	7.9	3.76×10^{20}		RS	[13]
CdO	10^2	1–10	$3–5\times10^{16}$		DCRS	[16]
CdO	$2–5\times10^{-3}$	12–15	10^{20}	2.4–2.42	IBS/SP	[6]
CdO	$2–5\times10^{-4}$	3–135	$0.2–5\times10^{20}$		ARE	[8]
CdO	$\sim10^{-3}$			2.2	CBD and Ann	[7]
CdO	6.6×10^{-3}	68	1.4×10^{19}	2.32	SP	[5]
CdO	1.4×10^{-3}	19	2.3×10^{20}	2.5	SP	[4]
CdO	2×10^{-3}	20	1.5×10^{20}	2.3–2.52	SP	[24]
CdO	$2.6–6.6\times10^{-4}$	576–100.5	$1.6–2.3\times10^{20}$	2.5–2.68	DCRMS	[10]
CdO	2.6×10^{-3}	1.59	1.49×10^{20}	2.58	RFS	[25]
CdO	2×10^{-2}			2.59	SG	[12]
CdO:Cu	9.4×10^{-3}	3.2	2.08×10^{20}		RS	[13]
CdO:In	5.3×10^{-3}	2.3	5.12×10^{20}		RS	[13]
CdO:F	6.7×10^{-4}	25.4	3.66×10^{20}	2.44	SP	[26]
CdO:Sn	2.1×10^{-4}	12.8	2.24×10^{21}	3.0	MOCVD	Present work
CdO:Sn	1.4×10^{-4}	24.2	1.8×10^{21}	3.2	MOCVD and He Ann	Present work
CdO:Sn	1.4×10^{-4}	11.3	3.34×10^{21}	3.35	MOCVD and H_2 Ann	Present work

[a] RS is relative sputtering. IBS is ion-beam sputtering, SP is spray pyrolysis, ARE is activated reactive evaporation, Ann is annealing, DCRMS is direct current reactive magnetron sputtering, RFS is radio frequency sputtering, and SG is sol–gel.

annealing. After He annealing, the electron mobility nearly doubled the value before annealing while the carrier concentration decreased by 20–30%, resulting in an almost twofold improvement in conductivity. The higher mobility was possibly due to the enhanced crystallinity after annealing as observed from the XRD measurement [27]. Annealing in H_2 ambient resulted in a 40–50% increase in the carrier concentration compared to the one before annealing; the mobility remained nearly unchanged. The larger oxygen deficiency after H_2 annealing is believed to be the major cause of the higher carrier concentration.

4. Conclusions

Tin-doped cadmium oxide films have been deposited by atmospheric MOCVD. The electrical and optical properties of the films have been characterized. A sheet resistance in the range of 10–20 Ω/sq and transmission of 80–95% were obtained at a substrate temperature of 250 °C and a film thickness of 100–200 nm. The high conductivity of the films was mainly due to their extremely high carrier concentration of $2–3\times10^{21}/cm^3$ and moderate mobility of 10–15 $cm^2/V\,s$. The fabricated films exhibited high optical bandgaps of 3.0–3.2 eV corresponding to direct band-to-band transition, and 2.5–2.6 eV corresponding to indirect band-to-band transition. Film properties were further improved by post-deposition annealing, and a state-of-the-art resistivity value of $1.4–1.6\times10^{-4}$ Ω cm and the highest optical bandgap of 3.35 eV ever reported for the CdO films have been demonstrated.

Acknowledgments

This work was supported by the National Renewal Energy Laboratory.

References

[1] V.K. Jain, A.P. Kulshreshta, Sol. Energy Mater. 4 (1981) 151.
[2] R.G. Gordon, MRS Bull. 25 (2000) 52.
[3] K. Bädeker, Ann. Phys. Lpz. 22 (1907) 749.
[4] K. Gurumurugan, D. Mangalaraj, Sa.K. Narayandass, C. Balasubramanian, Phys. Stat. Sol. (a) 143 (1994) 85.
[5] K. Gurumurugan, D. Mangalaraj, Sa.K. Narayandass, K. Sekar, C.P.G. Vallabhan, Semicond. Sci. Technol. 9 (1994) 1827.
[6] T.L. Chu, S.S. Chu, J. Electron. Mater. 19 (1990) 1003.
[7] M. Ocampo, P.J. Sebastian, J. Campos, Phys. Stat. Sol. (a) 143 (1994) K29.
[8] G. Phatak, R. Lal, Thin Solid Films 245 (1994) 17.
[9] I.J. Ferrer, Electrochim. Acta 38 (1993) 2199.
[10] K. Gurumurugan, D. Mangalaraj, Sa.K. Narayandass, J. Electron. Mater. 25 (1996) 765.
[11] T.K. Subramanyam, S. Uthanna, B.S. Naidu, Physica Scripta 57 (1998) 317.
[12] D.M. Carballeda-Galicia, R. Castanedo-Pérez, O. Jiménez-Sandoval, S. Jiménez-Sandoval, G. Torres-Delgado, C.I. Zúñiga-Romero, Thin Solid Films 317 (2000) 105.
[13] T.K. Lakshmanan, J. Electrochem. Soc. 110 (1963) 548.
[14] Z. Zhao, D.L. Morel, C.S. Ferekides, 16th European Photovoltaic Solar Energy Conference, Vol. 1, Glasgow, UK, May 1–5, 2000, p. 808.
[15] G.B. Williamson, R.C. Smallman, Phil. Mag. 1 (1956) 34.
[16] K. Tanaka, A. Kunioka, Y. Sakai, Jpn J. Appl. Phys. 8 (1969) 681.
[17] K. Maschke, U. Rossler, Phys. Stat. Sol. 28 (1968) 577.
[18] S. Tewari, Solid State Commun. 12 (1973) 437.
[19] A. Breeze, P.G. Perkins, Solid State Commun. 13 (1973) 1031.
[20] R. Kondo, H. Okhimura, Y. Sakai, Jpn J. Appl. Phys. 10 (1971) 1547.

[21] H. Finnkenrath, H. Kohler, M. Lochmann, Z. F. Angew. Phys. 21 (1966) 512.
[22] P.A. Wolff, Phys. Rev. 126 (1962) 405.
[23] A.J. Nozik, Phys. Rev. B 6 (1972) 453.
[24] C. Sravani, K.T.R. Reddy, P.S. Reddy, P. Jayarama Reddy, J. Mater. Sci. Lett. 13 (1994) 1045.
[25] N. Ueda, H. Maeda, H. Hosono, H. Kawazoe, J. Appl. Phys. 84 (1998) 6174.
[26] R. Ferro, J.A. Rodriguez, Thin Solid Films 347 (1999) 295.
[27] Z. Zhao, V. Komin, V. Viswanathan, D.L. Morel, C.S. Ferekides, Proceedings of 28th IEEE Photovoltaic Specialists Conference, Anchorage, AK, September 15–22, 2000, p. 662.